Efficient polynomial expansion of the scattering Green's function: Application to the D+H2(v=1) rate constant

Scott M. Auerbach and William H. Miller

Citation: The Journal of Chemical Physics **100**, 1103 (1994); doi: 10.1063/1.466642
View online: http://dx.doi.org/10.1063/1.466642
View Table of Contents: http://scitation.aip.org/content/aip/journal/jcp/100/2?ver=pdfcov
Published by the AIP Publishing

Efficient polynomial expansion of the scattering Green's function: Application to the $D+H_2(v=1)$ rate constant

Scott M. Auerbach[a] and William H. Miller[b]
Department of Chemistry, University of California, and Chemical Sciences Division, Lawrence Berkeley Laboratory, Berkeley, California 94720

(Received 13 September 1993; accepted 6 October 1993)

We apply the absorbing boundary condition (ABC) discrete variable representation (DVR) theory of quantum reactive scattering to the initial state selected $D+H_2(v=1, j)\rightarrow DH+H$ reaction. The ABC-DVR Green's function is efficiently computed by a Newton polynomial expansion. We compute accurate reaction probabilities for the total energies and angular momenta required to obtain the thermal rate constants $k_{v=1,j}(T)$. At $T=310$ K, a thermal average over $j=(0,1,2,3)$ is performed to yield the final result $k_{v=1}(310\ \text{K})=1.87\times10^{-13}$ cm^3 molecule^{-1} s^{-1}, in *quantitative* agreement with the most recent experimental value $(1.9\pm0.2)\times10^{-13}$ cm^3 molecule^{-1} s^{-1}. The J-shifting approximation using accurate $J=0$ reaction probabilities is tested against the exact results. It reliably predicts $k_{v=1}(T)$ for temperatures up to 700 K, but individual $(v=1, j)$ selected rate constants are in error by as much as 41%.

I. INTRODUCTION

The past few years in chemical reaction dynamics have seen several detailed and reliable comparisons between experiment and theory.[1–4] These comparisons have brought to light important new concepts, e.g., the signature of resonances in angular distributions[5] and the role of the geometric phase in chemical reactions.[4] The ability to carry out numerically exact reactive scattering calculations has been crucial in these studies, helping to interpret the experimental data and to ensure that our picture of the chemical reaction is complete. At present, though, exact reactive scattering calculations have been restricted to three-atom systems.[6,7] There is great impetus for methodological development, potentially allowing the exact treatment of experimentally[8] and technologically important four-atom systems. Thus, the present study focuses on the development and application of efficient techniques in quantum reactive scattering theory.

Several approaches for exact reactive scattering calculations are currently available.[6] By construction, most of these involve determining the state-to-state scattering amplitudes. In extending exact theory to larger systems, it may not be appropriate (or possible) to study chemical reactions in such detail. Indeed, a theoretical framework based on the *direct* calculation of averaged reaction probabilities should be more applicable to larger systems. The absorbing boundary condition (ABC) formulation of quantum reactive scattering theory provides such a framework, allowing the direct calculation of the cumulative,[9,10] initial state selected,[11,12] and state-to-state reaction probabilities.[12,13] In this article, we employ the initial state selected perspective, which directly gives the probability for reaction from a single reactant state to all open product states. This is especially relevant, since most modern experiments which state select reactants involve a small number of reactant states.

The ABC method reduces the scattering problem to the determination of the ABC Green's function (**G**), a matrix inverse. Although formally this is just as computationally demanding as full diagonalization, the initial state selected formalism only requires a single column of **G**. Iterative methods,[14] which require very little core memory, can be used to rapidly compute a single column of **G**. In particular, we have developed an iterative method especially suited for the calculation of **G**, and previously described by one of us.[15] It evaluates **G** as the half-Fourier transform of the propagator, which is accurately represented in a Newton polynomial expansion.[16,17] The Newton algorithm is extremely robust and efficient. As we will show, we are able to converge initial state selected reaction cross sections for $D+H_2$ using the Newton method in 10 min on an IBM RS/6000.

An important and nontrivial application of the ABC initial state selected formalism is the calculation of the $D+H_2(v=1)$ rate constant. This quantity has received much attention in an attempt to resolve a fairly large discrepancy between experiment[18–21] and theory,[22–29] with the experimental results typically being one or two orders of magnitude larger than the theoretical ones. Surprisingly, the experimental rate constants varied much more from group to group than did the theoretical ones. In particular, Glass and Chaturvedi[19] accounted for one order of magnitude in the discrepancy by preparing $H_2(v=1)$ without recourse to vibrationally excited HF, which was thought to contribute indirectly to the detected population of H atoms in the experiment of Keuba *et al.*[18] Dreier and Wolfrum[21] accounted for roughly another order of magnitude by using coherent anti-Stokes Raman scattering (CARS) spectroscopy to directly monitor most of the reagents in the system. The most accurate theoretical treatment of this rate constant is by Zhang and Miller,[30] using the S-matrix version of the Kohn variational principle. However, they reported the rate constant for $D+H_2(v=1, j=0)$, and the

[a]Present address: Department of Chemistry, University of California at Santa Barbara, Santa Barbara, CA 93106.
[b]Author to whom correspondence should be addressed.

 0021-9606/94/100(2)/1103/10/$6.00

experiment by Dreier and Wolfrum involved a thermal distribution of reactant j states. With the extreme importance of fundamentally understanding the role of vibrational excitation in chemical reactions, we undertook the calculation of this rate constant with the present initial state selected formalism. We will show that quantitative agreement has now been obtained.

As important as exact reactive scattering calculations may be, approximations are indispensable in developing useful tools for estimating the reactivity of complex systems. An important model is the J-shifting approximation (JSA),[31–33] which allows one to estimate observables such as cross sections and rate constants when only $J=0$ calculations are possible. It does so by ignoring the Coriolis coupling, and by assuming that the centrifugal coupling is only important near the transition state geometry. The accuracy of the JSA was tested by Bowman,[31] who examined the $J=4$ partial cumulative reaction probability for $H+H_2$. He found excellent agreement with the exact results of Chatfield *et al.*[34] up to total energy $E\cong 1.2$ eV. In addition, Takada *et al.*[35] used the JSA to compute cross sections and rate constants for $D+H_2(v=j=0)$. Comparing to the exact results of Zhang and Miller,[30] they too found excellent agreement for low enough energy. However, the JSA has never been tested in the important case of an initial state selected reaction with rovibrationally excited reactants. This is particularly significant in developing estimates of reaction rates to compare with the state and bond selected experiments of Crim and co-workers,[8] and Zare and co-workers.[36] In the present study, we test the JSA in the calculation of $D+H_2(v=1, j)$ rate constants. We will show that the JSA is qualitatively correct when selecting individual j states, and is semiquantitative once the rate constants are thermally averaged over the j states.

The remainder of the paper is presented as follows. Section II describes the general methodology used in these calculations. Section III defines the basis and the asymptotic boundary conditions. We discuss the results in Sec. IV, and conclude in Sec. V.

II. GENERAL METHODOLOGY

We now discuss the formalism used in the present study to obtain the initial state selected rate constant for an atom–diatom reaction. We briefly review the general rate constant formulas, the ABC method of obtaining reaction probabilities, and the Newton polynomial algorithm for the ABC-DVR Green's function.

A. General rate constant formulas

The quantity of experimental interest is the thermal rate constant with initial vibrational state selection $k_v(T)$. This corresponds to a rate measurement of the total yield of a reaction where all the motions of the reactants are in thermal equilibrium at temperature T, except for the diatomic vibration. The latter is promoted to a nonequilibrium state by laser excitation. This rate constant can be obtained from averaging the more detailed (v, j) selected rate constant via

$$k_v(T)=\sum_{j=0}^{\infty} p_{v,j}(T)k_{v,j}(T), \tag{2.1}$$

where

$$p_{v,j}(T)=\frac{(2j+1)w_j e^{-\epsilon_{v,j}/k_BT}}{\Sigma_{j'=0}^{\infty}(2j'+1)w_{j'}e^{-\epsilon_{v,j'}/k_BT}} \tag{2.2}$$

is the rotational distribution of reactant diatomics in the vibrational state v. In Eq. (2.2), $\epsilon_{v,j}$ is the reactant diatomic rovibrational energy, k_B is Boltzmann's constant, and w_j accounts for any symmetry statistics of the reactant diatomic (e.g., for H_2, $w_j=1$ for even j, and 3 for odd j). We note that there is also an average over m_j, the projection quantum number of j, which is discussed below.

The reaction of a diatomic molecule in state (v, j) with an atom approaching with thermal velocities has a rate constant given by[37]

$$k_{v,j}(T)=\sqrt{\frac{8k_BT}{\pi\mu_t}}(k_BT)^{-2}\int_0^{\infty} dE_t\, E_t e^{-E_t/k_BT}\sigma_{v,j}(E_t), \tag{2.3}$$

where E_t is the initial translational energy of the reactants, and μ_t is the translational reduced mass. The initial state selected reaction cross section $\sigma_{v,j}(E_t)$ can be obtained from quantum-mechanical reaction probabilities by partial wave expansion,[37] in which

$$\sigma_{v,j}(E_t)=\frac{\pi}{k_t^2}\sum_{J=0}^{\infty}\frac{2J+1}{2j+1}\sum_{l=|J-j|}^{J+j}P^J_{v,j,l}(E_t), \tag{2.4}$$

where k_t is the translational wave vector associated with E_t and μ_t. We perform the average over m_j by averaging the space-fixed reaction probabilities over l, the orbital angular momentum quantum number. In Eq. (2.4), $P^J_{v,j,l}(E_t)$ is the initial state selected reaction probability defined by

$$P^J_{v,j,l}(E_t)\equiv\sum_{\{v',j',l'\}}P^J_{v',j',l'\leftarrow v,j,l}(E), \tag{2.5}$$

where $\{v', j', l'\}$ is the open channel space of *products* at total energy $E=E_t+\epsilon_{v,j}$, and $P^J_{v',j',l'\leftarrow v,j,l}(E)$ are the state-to-state reaction probabilities. The reaction probability in Eq. (2.5) is the fundamental quantity of interest which we obtain with the ABC formalism reviewed below.

B. ABC formulation of quantum reactive scattering

The ABC approach to quantum reactive scattering was originally derived to compute the cumulative reaction probability.[9,10] It was then applied to the calculation of initial state selected and state-to-state reaction probabilities.[12] Thorough discussions of the theory can be found in these references. For completeness, a brief outline of the formulas relevant for atom–diatom reactions is provided below.

We use ABC to achieve two related goals.[11,38–40] First, by absorbing all outgoing flux the scattering problem is converted into an effective non-Hermitian bound state problem, in which standard L^2 basis set techniques may be used. Second, by placing the absorbing potentials very close to the interaction region, some[11,12] or all[9] of the as-

ymptotic state information can be implicitly averaged, facilitating more economical calculations. In this spirit, the ABC initial state selected reaction probability is given by[12]

$$P^J_{v,j,l}(E_t)=\frac{2}{\hbar}\langle\Psi^J_{v,j,l}(E_t)|\hat{\epsilon}_p|\Psi^J_{v,j,l}(E_t)\rangle, \tag{2.6}$$

where $\hat{\epsilon}_p$ is the absorbing potential operator in the product region of configuration space. In Eq. (2.6), $|\Psi^J_{v,j,l}(E_t)\rangle$ is the ABC scattering wave function defined by

$$|\Psi^J_{v,j,l}(E_t)\rangle\equiv\hat{G}^{\rm ABC}(E)i\hat{\epsilon}|\Phi^J_{v,j,l}(E_t)\rangle, \tag{2.7}$$

where the ABC Green's function is given by

$$\hat{G}^{\rm ABC}(E)=(E+i\hat{\epsilon}-\hat{H})^{-1}. \tag{2.8}$$

In Eq. (2.7), $\hat{\epsilon}$ is the absorbing potential operator for all chemical arrangements and $|\Phi^J_{v,j,l}(E_t)\rangle$ is a reference scattering state with incoming-wave boundary conditions in channel (v,j,l,J,E_t). In what follows, we omit the "ABC" superscript with the understanding that we are using the ABC formulation.

We note that use of an absorbing potential in Eq. (2.8) in the definition of the Green's function is tantamount to replacing the infinitesimal energy ϵ that arises in formal scattering theory with a coordinate dependent function $\epsilon(q)$. This replacement is valid as long as $\epsilon(q)$ is negligible in the strong chemical interaction region, and absorbs all flux by the edge of the L^2 basis.

The ABC formulation reduces the scattering problem to the computation of the ABC Green's function. We have developed an efficient algorithm for this purpose,[15] which we now discuss.

C. The Newton algorithm for the ABC-DVR Green's function

A finite basis representation of Eq. (2.7) gives

$$\Psi^J_{v,j,l}(E_t)=\mathbf{G}(E)i\epsilon\Phi^J_{v,j,l}(E_t) \tag{2.9}$$

which can be viewed as the solution of a non-Hermitian linear system of simultaneous equations. With the intent to apply this formalism to large systems, we use a discrete variable representation[41–43] (DVR), resulting in a sparse Hamiltonian matrix in a multidimensional system. The computational problem is to be able to solve the very large, sparse linear system as efficiently as possible.[44] We have developed an algorithm for solving Eq. (2.9) which is fast, stable, and uses minimal core memory. We will give a brief outline of the method, which is described more thoroughly in Ref. 15. It is based on representing $\mathbf{G}(E)$ as the half-Fourier transform of the ABC propagator, which is obtained by Newton polynomial expansion.[17]

We begin with the Fourier integral representation of the ABC Green's function:

$$\mathbf{G}(E)=(i\hbar)^{-1}\int_0^\infty dt\, e^{i(E+i\epsilon-\mathbf{H})t/\hbar}. \tag{2.10}$$

Because the magnitude of ϵ is finite in the ABC formulation, this integral converges in finite time (as opposed to the infinite time required by formal scattering theory). It was shown in Ref. 15 how to automate the choice of this finite time *a priori*. This form for $\mathbf{G}(E)$ is advantageous because it allows us to work directly with the time propagator, for which the Chebyshev polynomial expansion[45] is the method of choice for many problems in chemical physics. However, in the present case the Chebyshev expansion would become unstable because of the ABC. Following the work of Berman *et al.*[17] we expand the ABC propagator in Newton polynomials,[16] which remain stable regardless of the absorbing potential. The application of Newton polynomials to chemical physics is beautifully discussed in Ref. 17. We will review those aspects most relevant to the present study.

Newton polynomials arise from the theory of interpolation in the complex plane. Indeed, we suppose an analytic function $f(z)$ is known at a set of complex support points $\{(z_k,f_k)\}$ where $f_k=f(z_k)$. An approximate representation of f in the vicinity of the sampling points $\{z_k\}$ is given by

$$f(z)\cong P_{K_{\rm newt}}(z),$$

where

$$P_{K_{\rm newt}}(z)\equiv\sum_{k=0}^{K_{\rm newt}}a_kR_k(z). \tag{2.11}$$

In Eq. (2.11), $R_k(z)$ is the Newton polynomial of degree k defined by

$$R_k(z)\equiv\begin{cases}1 & k=0\\ \Pi_{j=0}^{k-1}(z-z_j) & k>0\end{cases}, \tag{2.12}$$

and a_k is the kth divided difference coefficient,[46] determined by requiring that $P_k(z_k)=f_k$ for each k. As such, the coefficients $\{a_k\}$ are built up iteratively, in a way which can be summarized by

$$a_0=f_0,\quad a_1=\frac{f_1-f_0}{z_1-z_0},\ldots$$

and in general for $k>0$,

$$a_k=\frac{f_k-P_{k-1}(z_k)}{R_k(z_k)}. \tag{2.13}$$

The numerical details of how to choose optimal sampling points are amply discussed in Ref. 17. Our procedure, which is most relevant for quantum scattering applications, is given in Ref. 15.

To expand the ABC propagator in Newton polynomials, it is more numerically stable if we shift and scale the Hamiltonian. We first define the non-Hermitian matrix $\tilde{\mathbf{H}}\equiv\mathbf{H}-i\epsilon$. We then rewrite the ABC propagator as

$$e^{-i\tilde{\mathbf{H}}t/\hbar}=e^{-i\langle\tilde{\mathbf{H}}\rangle t/\hbar}e^{-i\mathbf{Z}\tau}, \tag{2.14}$$

where

$$\mathbf{Z}=\frac{\tilde{\mathbf{H}}-\langle\tilde{\mathbf{H}}\rangle}{\Delta(\tilde{\mathbf{H}})/2}. \tag{2.15}$$

In Eqs. (2.14) and (2.15), the following quantities are:

$$\tau = t\Delta(\tilde{\mathbf{H}})/2\hbar,$$

$$\langle\tilde{\mathbf{H}}\rangle = [\mathrm{Re}(\lambda_{\max}) + \mathrm{Re}(\lambda_{\min})]/2,$$

$$\Delta(\tilde{\mathbf{H}})/2 = \max\{|\lambda_{\max} - \langle\tilde{\mathbf{H}}\rangle|, |\lambda_{\min} - \langle\tilde{\mathbf{H}}\rangle|\},$$

where $\lambda_{\max}$ and $\lambda_{\min}$ are the (complex) eigenvalues of $\tilde{\mathbf{H}}$ with largest and smallest real part, respectively. In the case of a positive definite Hamiltonian matrix $\mathbf{H}$, where $|\lambda_{\min}| \cong 0$, the above relations simplify to $\langle\tilde{\mathbf{H}}\rangle = \Delta(\tilde{\mathbf{H}})/2 = \mathrm{Re}(\lambda_{\max})/2$. In practice, $\lambda_{\min}$ and $\lambda_{\max}$ are determined with a low-order Lanczos calculation.[47]

In actual calculations, $e^{-i\mathbf{Z}\tau}$ is the matrix which is expanded in Newton polynomials according to

$$e^{-i\mathbf{Z}\tau} \cong \sum_{k=0}^{K_{\mathrm{newt}}} a_k(\tau) R_k(\mathbf{Z}), \tag{2.16}$$

and Eqs. (2.11)–(2.13).

III. DEFINING THE LINEAR SYSTEM

We define the precise linear system to be solved in Eq. (2.9) for the $D+H_2$ quantum reactive scattering calculations. This entails the choice of system coordinates, basis set, asymptotic state, and absorbing potential. We note that, with respect to the coordinates and basis set, much of our work parallels that of Choi and Light[48] in their calculations on the Ar–HCl van der Waals complex.

A. The coordinates

We use the mass-scaled (MS) body-fixed Jacobi coordinates of the reactant $D+H_2$ to define the differential Hamiltonian operator. The internal coordinates are $\mathbf{q}=(r,R,\gamma)$, where r is the MS bond length of H_2, R is the MS scattering coordinate, and γ is the bending angle. This choice seems reasonable because the initial state selection requires that more grid points be placed in the reactant region. Also, the use of body-fixed coordinates allows for more economical exact calculations (*vide infra*).[49,50] After integrating out the Euler angles with a basis of parity-adapted Wigner functions,[48,51] the Hamiltonian becomes

$$\begin{aligned}\hat{H}^{JP}_{K',K}(r,R,\gamma) = \delta_{K',K}\Big\{ & \hat{T}^r + \hat{T}^R + \hat{T}^\gamma + \frac{\hbar^2}{2\mu R^2} \\ & \times [J(J+1) - 2K^2] + \hat{V}(r,R,\gamma)\Big\} \\ & - \delta_{K',K+1}\Big\{(1+\delta_{K,0})^{1/2} \frac{\hbar}{2\mu R^2} \Lambda^+_{JK} \hat{j}^+\Big\} \\ & - \delta_{K',K-1}\Big\{(1+\delta_{K,1})^{1/2} \frac{\hbar}{2\mu R^2} \Lambda^-_{JK} \hat{j}^-\Big\},\end{aligned} \tag{3.1}$$

where the system mass is

$$\mu = \left(\frac{M_D M_H M_H}{M_D + M_H + M_H}\right)^{1/2} = 1298.796 \text{ a.u.}$$

The inversion symmetry quantum number P determines the range of K' and K, i.e., when $J+P$ is even $K',K=0,\ldots,J$ and otherwise $K',K=1,\ldots,J$. In Eq. (3.1), the following quantities are:

$$\begin{aligned}\hat{T}^r &= -\frac{\hbar^2}{2\mu}\frac{\partial^2}{\partial r^2}, \\ \hat{T}^R &= -\frac{\hbar^2}{2\mu}\frac{\partial^2}{\partial R^2}, \\ \hat{T}^\gamma &= \frac{1}{2\mu}\left(\frac{1}{r^2} + \frac{1}{R^2}\right)\hat{j}^2, \\ \Lambda^\pm_{JK} &= \sqrt{J(J+1) - K(K\pm 1)}.\end{aligned} \tag{3.2}$$

Also, $\hat{j}^\pm$ are the usual raising and lowering operators for the diatomic angular momentum in the body-fixed system, and $\hat{V}(r,R,\gamma)$ is the Liu–Siegbahn–Truhlar–Horowitz (LSTH)[52–54] potential energy surface (PES).

B. The basis set

In the present study we use a DVR[41–43] for each internal degree of freedom. The DVR gives a diagonal potential matrix, and thus, all the coupling is in the one-dimensional kinetic energy matrices. This is a poor, but convenient representation because the multidimensional Hamiltonian matrix is sparse, which facilitates iterative calculations based on the sparse matrix–vector multiply.[55,56] In practice, we first define a direct product grid in four dimensions, called the primitive grid. This is then truncated based on several criteria to give the final grid used to represent the ABC wave function. First, we discuss the construction of the primitive grid, and the relevant kinetic energy matrix elements. We then discuss the truncation algorithm.

For the two radial coordinates, we use the radial sinc DVR given by Colbert and Miller.[57] Considering the scattering coordinate first, a grid of R values is defined by $R_i = i\Delta R$ where $i=1,2,3,\ldots$. The point at zero is automatically deleted because of the Jacobian weight at the origin. The radial kinetic energy matrix element is

$$T^R_{ii'} = \frac{\hbar^2}{2\mu\Delta R^2}(-1)^{i-i'}\begin{cases} \pi^2/3 - 1/2i^2, & i=i' \\ \dfrac{2}{(i-i')^2} - \dfrac{2}{(i+i')^2}, & i\neq i' \end{cases}. \tag{3.3}$$

The same applies for the r coordinate, except with the vibrational grid spacing Δr. In practice, we have used the same grid spacing for the two radial coordinates, because they are associated with the same mass μ. The grid spacing is chosen by requiring that the number of points per de Broglie wavelength (N_B) is roughly 4, as was found by Colbert and Miller.[57]

For the bending angle, we use an associated Legendre (AL) DVR which properly removes the singularity in the Hamiltonian for collinear geometries when $K>0$. We sym-

metrize the AL DVR to exploit the exchange symmetry of the two identical H atoms, allowing us to use half as many angular grid points.

For simplicity, we use a K-independent grid.[58,59] That is, we obtain grid points $\{x_i\}$ and weights $\{w_i\}$ for the $K=0$ AL functions (i.e., the usual Gauss–Legendre DVR). We then use these points and weights to construct the angular kinetic energy for all values of K in the Hamiltonian. This is to be contrasted with the treatment of Choi and Light[48] who use different points and weights for each K block. Both approaches are valid, and we wanted to keep the basis set as simple as possible.

Using $N_{\rm AL}$ symmetrized AL DVR states, and labeling the exchange symmetry blocks by $p=0$ or 1, the (p,K)-dependent angular kinetic energy matrix elements are given by

$$j^2_{ii'}(p,K)=\sum_{j=K}^{2N_{\rm AL}-1} s_j(p)\{\sqrt{w_i}P^K_j(x_i)[\hbar^2 j(j+1)] \times P^K_j(x_{i'})\sqrt{w_{i'}}\}. \tag{3.4}$$

With the phase convention that $P^K_j(\cos\gamma) = \sqrt{2\pi}Y_{jK}(\gamma,0)$, where $Y_{lm}(\theta,\phi)$ is the usual spherical harmonic,[46] the symmetry factor $s_j(p)$ is given by $s_j(p) =[1+(-1)^{j+p}]$. Furthermore, after applying the $\delta_{K',K+1}$ Kronecker delta, the $\hat{j}^+$ operator in this basis becomes

$$j^+_{ii'}(p,K)=\sum_{j=K+1}^{2N_{\rm AL}-1} s_j(p)\{\sqrt{w_i}P^{K+1}_j(x_i) \times[\hbar\Lambda^+_{jK}]P^K_j(x_{i'})\sqrt{w_{i'}}\}. \tag{3.5}$$

To complete the definition of the basis set, we note that $j^-_{ii'}(p,K) = j^+_{i'i}(p,K-1)$.

The primitive grid is truncated in the following fashion. For each DVR grid point in the primitive grid, a diagonal element of

$$\hat{T}^\gamma+\frac{\hbar^2}{2\mu R^2}J(J+1)+\hat{V}(r,R,\gamma)$$

is constructed. If that energy exceeds some input $V_{\rm cut}$, the point is discarded; otherwise it is retained in the basis.[60] Also, if a point is asymptotic, based on some convergence criterion related to the definition of the ABC, it is also discarded. In this way, the grid is tailored to the shape of the PES and the ABC. The sparse matrix–vector multiply with a truncated DVR grid was first discussed by Groenenboom *et al.*,[55,56] and their method is adopted here.

To complete the definition of the truncated basis set, we consider the allowed values of K, the body-fixed projection quantum number. In principle $K=0,\ldots,J$ for even $J+P$ and $1,\ldots,J$ for odd $J+P$. With a finite basis for the Jacobi angle, however, K cannot exceed $\min(J,2N_{\rm AL}-1)$. We have found that for the reaction probabilities considered in the present study, convergence is reached with $K_{\max}=2$, in accord with the basis set contraction results of Zhang.[50] This rapid convergence with respect to $K_{\max}$ facilitates exact calculations with very modest increases in CPU time as J increases, and is one of the many useful aspects of the body-fixed representation.

C. The reference scattering state

The reference scattering state can be chosen as a distorted wave (with any level of distortion) or as a free wave, as long as it is regular at the origin and is an eigenstate of the asymptotic Hamiltonian, $\hat{H}_0=\lim_{R\to\infty}\hat{H}$. Groenenboom *et al.*[56] and Thompson and Miller[12] have found it very useful to use inelastically distorted waves in their reactive scattering calculations, because they could represent the chemical reaction by focusing on the local exchange region. For the simplicity of the present application we use (almost) free waves, including only the centrifugal phase shift. This is the lowest level of distortion which facilitates practical calculations.

With this level of distortion, the reference scattering state is the product of a translational state, a vibrational state, and a rotational state:

$$|\Phi^J_{v,j,l}(E_t)\rangle=|h_l(E_t)\rangle|\phi_{v,j}\rangle|\mathscr{Y}^J_{j,l}\rangle. \tag{3.6}$$

For the translational function, we choose the spherical Hankel function of the second kind $\{h^{(2)}_l(x)\}$,[46] properly normalized to give unit incoming flux;

$$\langle R|h_l(E_t)\rangle\equiv\frac{-ikR}{\sqrt{v_t}}h^{(2)}_l(kR)\sim\frac{1}{\sqrt{v_t}}e^{-i(kR-l\pi/2)}. \tag{3.7}$$

In Eq. (3.7), $k=\sqrt{2\mu E_t}/\hbar$ and $v_t=\hbar k_t/\mu_t$, where μ_t and k_t are defined in Eqs. (2.3) and (2.4), respectively. We note that these are the same incoming-wave boundary conditions used in many of the S-matrix Kohn variational principle calculations.[30] Also, in Eq. (3.6), $|\phi_{v,j}\rangle$ is the diatomic rovibrational state.

The rotational state $|\mathscr{Y}^J_{j,l}\rangle$ in Eq. (3.6) is a space-fixed (SF) coupled eigenstate of $\hat{J}^2$, $\hat{J}_{Z_{SF}}$, $\hat{j}^2$, and $\hat{l}^2$. (Without loss of generality we suppress the space-fixed projection quantum number M in $|\mathscr{Y}^{J,M}_{j,l}\rangle$.) This asymptotic rotational state is used in most modern reactive scattering calculations.[61] It is useful for three reasons. First, it exploits the fact that J is conserved. Second, in the ABC formulation of quantum scattering, the absorbing potential may be nonzero only for values of R large enough that the asymptotic state nearly solves the Schrödinger equation. The term in the Hamiltonian which is responsible for mixing l states is the PES, which is typically a much shorter ranged interaction than the $1/R^2$ term which couples the body-fixed labels $\{m_j\}$. As such, the space-fixed representation allows the use of smaller L^2 basis sets. Third, the strength of the coupling which mixes the $\{m_j\}$ manifold increases as $\Lambda^{\pm}_{JK}\sim J$ [cf. Eqs. (3.1) and (3.2)], and as such would require reoptimization of the basis set and absorbing potential for each value of J. Thus, the space-fixed representation allows us to use a single, relatively small L^2 basis for all values of J.

To discuss the frame transformation and the use of symmetry in the present calculations, we indicate the transformation between a body-fixed rotational basis state and the space-fixed asymptotic rotational state. We label the body-fixed rotational basis state by $|JKPip\rangle$, where KP labels a symmetrized Wigner state with inversion symme-

try P, and ip labels a symmetrized AL DVR state with exchange symmetry p. The transformation is given by

$$\langle JKPip|\mathscr{Y}^J_{j,l}\rangle = \{\sqrt{w_i}P^K_j(x_i)\}\left\{\sqrt{\frac{2l+1}{2J+1}}\,C(jlK0|jlJK)\right\} \times\left\{\frac{1}{\sqrt{2}}\,[1+(-1)^{j+p}]\right\} \times\left\{\frac{1}{\sqrt{2(1+\delta_{K,0})}}\,[1+(-1)^{j+l+P}]\right\}. \tag{3.8}$$

The first factor in Eq. (3.8) is the usual DVR-FBR transformation element.[43] The second factor is the frame transformation, which is proportional to a Clebsch–Gordan coefficient.[51] The remaining factors demonstrate the relationship between the symmetry of the basis state and the asymptotic state. In particular, since the asymptotic state has both definite exchange and inversion symmetry, it projects onto the block of the Hamiltonian with exchange symmetry $p=j$ and inversion symmetry $P=j+l$. Using the proper symmetry blocks, these factors are $\sqrt{2}$ for $K=0$ and 2 for $K>0$, multiplying the reaction probability in Eq. (2.6) by 2 and 4, respectively. Thus, the $D+H_2$ initial state selection allows the calculation of properly symmetrized reaction probabilities while only explicitly treating $\sim\frac{1}{4}$ of the full Hamiltonian.

D. The absorbing potential

The optimum absorbing potential is one which absorbs all outgoing flux with negligible backreflection, as fast (in space) as possible. Several studies have sought reliable guidelines for determining optimal absorbing potentials.[40,62–65] We have found excellent convergence behavior with a quartic function:

$$\epsilon[z(\mathbf{q})] = \lambda\left[\frac{z-z_0}{z_{\max}-z_0}\right]^4, \tag{3.9}$$

where $z=\max[R_a,R_b(\mathbf{q}),R_c(\mathbf{q})]$, and (a,b,c) label the three chemical arrangements. The parameters $(\lambda,z_0,z_{\max})$ are different in different arrangements. They are set to give more gentle absorption in the reactant arrangement (a) than in the product arrangements (b,c), as demanded by the initial state selection. The parameter $z_{\max}$ determines the end of the grid in a particular arrangement. It is smaller in the product arrangements where no state selection is required. Converged values of these parameters will be reported below.

E. Summary of the methodology

With the vector $i\epsilon\Phi^J_{v,j,l}(E_t)$ now defined, we use the Newton method to apply $\mathbf{G}(E)$, thus giving the ABC scattering wave function and the reaction probability. The partial wave expansion and the Boltzmann average over relative translational energy and initial rotation give the desired rate constant.

TABLE I. Optimized convergence parameters for the present quantum reactive scattering calculations. These values are sufficient to give better than 3% accuracy for $E_t<0.37$ eV, and better than 6% accuracy otherwise. E=total scattering energy, Re is reactant, and Pr is product.

Absorbing potentials	
$\lambda^{Re}=1.8\times E$	$\lambda^{Pr}=1.0\times E$
$z_0^{Re}=4.5a_0$	$z_0^{Pr}=3.9a_0$
Primitive basis set	
$N_B=3.7$	$N_{AL}=7$
Truncated basis set	
$z_{max}^{Re}=(7.4\text{–}10.4)a_0$	$z_{max}^{Pr}=(5.5\text{–}8.5)a_0$
$V_{cut}=(2.5\text{–}4.2)$eV	$K_{max}=2$
Newton inversion	
$\tau=50$	$K_{newt}=80$
$\delta=2\times10^{-2}$	

IV. RESULTS AND DISCUSSION

We now present the results of our quantum reactive scattering calculations on the $D+H_2(v=1)$ system. As stated in the Introduction, the present study has two main goals. The first is to demonstrate the efficiency of the present method in a nontrivial application. For this purpose, we report the $D+H_2$ reaction cross sections $\sigma_{v=1,j}(E_t)$, in addition to the typical amounts of core memory and CPU time required for these calculations. The second objective is to determine the j and T dependence of $k_{v=1,j}(T)$, for the purpose of comparison with both experiment and approximate theory.

A. Cross sections

We have obtained converged reaction cross sections according to Eqs. (2.4) and (2.6). There are 13 convergence parameters to optimize. These fall into four roughly independent groups: ABC parameters $(\lambda^{Re},\lambda^{Pr},z_0^{Re},z_0^{Pr})$ for defining the absorbing potential [cf. Eq. (3.9)]; parameters (N_B,N_{AL}) for constructing the primitive basis; parameters $(z_{max}^{Re},z_{max}^{Pr},V_{cut},K_{max})$ for truncating the basis; and the Newton inversion parameters (K_{newt},τ,δ) defined in Ref. 15. Table I shows the optimized values. These parameters are sufficient to obtain better than 3% accuracy for the lower translational energies ($E_t<0.37$ eV), and better than 6% accuracy for the higher translational energies. We focus attention on the truncation parameters.

The parameters $(z_{max}^{Re},z_{max}^{Pr},V_{cut})$ require careful optimization. For small E_t, the initial translational energy z_{max}^{Re} and z_{max}^{Pr} must be large enough to encompass the long de Broglie wavelengths. Alternatively, for larger E_t, the parameter V_{cut} must be set to allow the wave function to sample larger portions of the PES. This competition between small and large translational energies caused the truncated grid sizes to be roughly independent of the energy, with grid sizes falling in the range $N_{grid}=6500\pm1500$.

Zhang has studied the convergence of partial cross sections with respect to K_{max}.[50] He found that the $J=10$ partial cross section for $H+H_2$ at total energy $E=0.6$ and 1.0 eV converges with $K_{max}=3$ and 4, respectively. In principle, the optimal value of K_{max} will depend on E and J, in

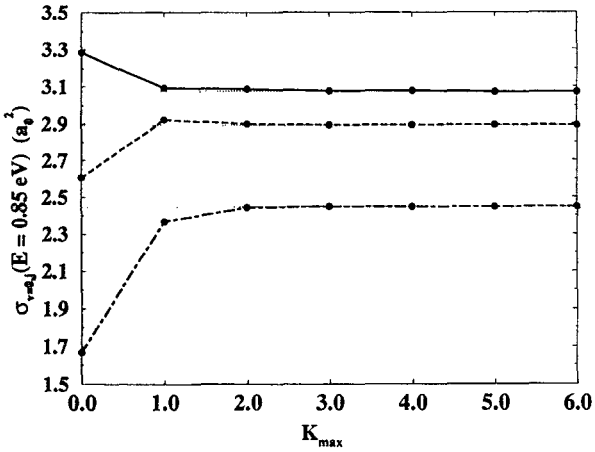

FIG. 1. Convergence with respect to K_{max} of the $D+H_2(v=0, j)$ reaction cross sections at total energy $E=0.85$ eV, for $j=(0,1,2)\mapsto$(*solid, dash, dot–dash*). We see rapid convergence as K_{max} increases, gaining nearly three digit accuracy for $K_{max}=2$. The $j=0$ calculation for $K_{max}=2$ required only 10 min.

addition to the initial rotational quantum number j. To avoid such complication, we examined the convergence of $D+H_2$ full cross sections with K_{max} for various values of E and j. Figure 1 shows the convergence of $\sigma_{v=0,j}$ at $E=0.85$ eV for $j=(0,1,2)$. We see rapid convergence of these cross sections as K_{max} increases, gaining nearly three digit accuracy with $K_{max}=2$. Similar results were obtained at $E=1.1$ eV, which require J as large as 24. Based on these results, we have used $K_{max}=2$ for all subsequent calculations reported in this study.

The $D+H_2(v=1,j)$ reaction cross sections are shown in Fig. 2, as a function of total energy [where $V(r=r_{eq}, R=\infty, \gamma)=0$ defines the zero of total energy]. The thick lines show the present calculations for $j=(0,1,2,3)$, and the thin dotted line is the $j=0$ result of Zhang and Miller obtained from the S-matrix version of the Kohn variational principle.[30] We see complete agreement for $j=0$ between the two methods over the entire energy range.

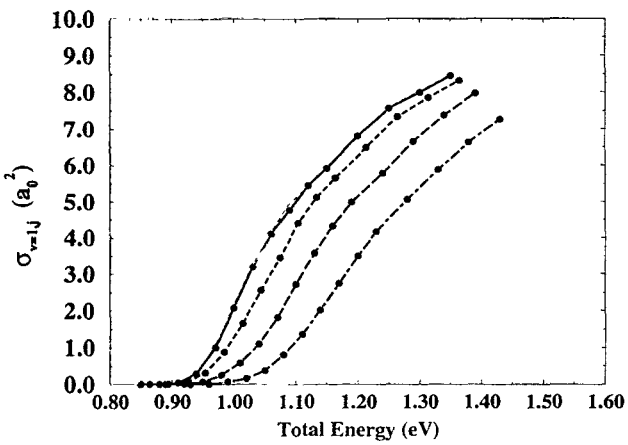

FIG. 2. Reaction cross sections for $D+H_2(v=1, j)$ as a function of total energy (eV). The thick lines show the present calculations for $j=(0,1,2,3)\mapsto$(*solid, dash, long-dash, dot–dash*), and the thin dotted line is the $j=0$ result of Zhang and Miller (Ref. 30) which agrees completely with the present calculations over the entire energy range. The cross sections decrease systematically with increasing j because of both symmetry and dynamics.

The initial state selected reaction cross sections in Fig. 2 demonstrate the very smooth energy dependence that results from averaging over partial waves and final states. We also see that the cross sections systematically decrease with increasing j. This results from two different effects. First, the $j>0$ cross sections involve an average over even and odd parity (P), whereas the $j=0$ cross sections arise from only even parity calculations. Since the odd parity block lacks the $K=0$ component, the transition state is not energetically accessible and the reaction probabilities are quite small. The second point is simply that, for $j=2$ and 3, the $J=0$ reaction probabilities are smaller than that for $j=0$ and 1.

We now report the computational effort required by these calculations, which were performed on an IBM RS/6000 Model 550. Total propagation times ranged from 60 (higher E_t) to 100 fs (lower E_t). This corresponds to the time required for reaction *and* absorption. The linear system size (i.e., the dimension of the Hamiltonian matrix) ranged from 5000 ($J=0$, small grid) to 25 000 ($J\geqslant 2$, large grid). The number of Newton expansions performed for each Green's function calculation varied from 10 to 20. With $K_{newt}=80$, this means 800–1600 matrix–vector multiples for each reaction probability.

All timings are for the $j=0$ cross sections. Timings for higher j values are roughly obtained by multiplying the $j=0$ timings by $2j+1$, the number of terms in the average over orbital angular momentum. The cross sections in Fig. 1 required $\sim 3\frac{1}{3}$ min times $K_{max}+1$, for a calculation using K_{max}. Thus, *converged reaction cross sections are obtained in 10 min.* The cross sections in Fig. 2 are more demanding, however, because the total energy is higher, and the initial translational energy is lower than that in Fig. 1. The lower energy cross sections and the very high energy cross sections in Fig. 2 required ~ 60 min per energy, and those at the intermediate energies required ~ 40 min per energy. Furthermore, with respect to core memory, *all* calculations presented required *less than* 4.5 Mbyte. This is possible because the Newton method is an iterative algorithm which is based on storing only a small number of vectors. Thus, these *very* modest memory and time requirements of the ABC-DVR Newton method suggest that it may be the most direct route to date for calculating accurate reaction cross sections.

B. Rate constants

We now present the results of our rate constant calculations using Eqs. (2.1)–(2.3). In this section we wish to emphasize two comparisons: the present theory vs experiment, and the present theory vs an approximate theory.

The theory we will test is the J-shifting approximation (JSA), made popular in quantum reactive scattering theory by Bowman[31,66] and Schatz.[67] The JSA assumes that K is conserved, and further that the centrifugal coupling is only important near the transition state geometry. Reac-

tion probabilities for $J,K>0$ are obtained by a (J,K)-dependent energy shift from the $J=0$ result via[31]

$$P^{J,K}_{v,j,l}(E_t) \cong P^{J=0}_{v,j,j}(E_t - \epsilon_{J,K}). \tag{4.1}$$

This allows one to estimate observables such as cross sections and rate constants when only accurate $J=0$ calculations are possible. As stated in the Introduction, Bowman[31] and Takada *et al.*[35] have examined the accuracy of the JSA, in both cases finding good agreement with exact results for low enough energy. The former study tested $H+H_2$ cumulative reaction probabilities for $J=4$, while the latter examined $D+H_2(v=j=0)$ cross sections and rate constants. Our calculation of exact $D+H_2[v=1, j=(0,1,2,3)]$ rate constants provides an interesting opportunity to test this approximation further.

In the present study, we will use the linear transition state JSA. This assumes contribution from $K=0$ only, and gives the following (v, j) selected rate constant:

$$k^{\mathrm{JSA}}_{v,j}(T) = \left[\sqrt{\frac{8k_BT}{\pi\mu_t}} (k_BT)^{-2} \frac{\hbar^2\pi}{2\mu_t} \right] \left(\frac{j+1}{2j+1} \right) Q^{\ddagger}_{\mathrm{rot}}(T) \times \int_0^{\infty} dE_t\, e^{-E_t/k_BT} P^{J=0}_{v,j,j}(E_t), \tag{4.2}$$

where

$$Q^{\ddagger}_{\mathrm{rot}}(T) = \sum_{J=0}^{\infty} (2J+1) e^{-B^{\ddagger}J(J+1)/k_BT}. \tag{4.3}$$

In Eq. (4.2), the factor of $j+1$ counts the number of l states in the sum over orbital angular momentum which contain a $K=0$ component. In Eq. (4.3), $B^{\ddagger}$ is the rotation constant of the linear transition state species, which is 8.6 cm^{-1} for the LSTH PES description of $D+H_2$. The above assumptions are expected to be satisfied at lower temperatures, but less so at higher temperatures.

We now consider experimental results for the $D+H_2(v=1)$ rate constant. As discussed in the Introduction, the measured rate constant for this reaction has been quite sensitive to the particular experimental procedure employed.[18–20] Dreier and Wolfrum[21] have measured the rate constant by applying CARS spectroscopy to monitor *directly* most of the reagents in the system. Since the other experiments involved indirect probing of some sort,[18–20] we consider the CARS measurement to be the most reliable. Thus, we take their result, $k_{v=1}(T=310\ \mathrm{K}) = (1.9\pm0.2) \times 10^{-13}\ \mathrm{cm}^3\ \mathrm{molecule}^{-1}\ \mathrm{s}^{-1}$, for comparison.

The most accurate theoretical treatment of this system is by Zhang and Miller,[30] who calculated the exact rate constant for $D+H_2(v=1, j=0)$. Their published result is $k_{v=1,j=0}(T=300\ \mathrm{K}) = 1.63\times10^{-13}\ \mathrm{cm}^3\ \mathrm{molecule}^{-1}\ \mathrm{s}^{-1}$. Although the j dependence of this rate constant is not expected to be too strong, a full description of the experiment requires a thermal average over j states. At $T=310$ K, $j=(0,1,2,3)$ accounts for 99.2% of the total population. We now present the results of an ABC-DVR calculation of these rate constants.

Table II shows $k_{v=1,j}(T=310\ \mathrm{K})$ with dimensions $10^{-13}\ \mathrm{cm}^3\ \mathrm{molecule}^{-1}\ \mathrm{s}^{-1}$, for $j=(0,1,2,3)$. Both exact partial wave expansion and JSA are shown for comparison,

TABLE II. Exact (EXA) and approximate (JSA) theoretical rate constants for $D+H_2(v=1, j)$ at $T=310$ K ($10^{-13}\ \mathrm{cm}^3\ \mathrm{molecule}^{-1}\ \mathrm{s}^{-1}$). Both EXA and JSA employ the ABC-DVR Newton method. However, the JSA uses only $J=0$ reaction probabilities, and approximates the partial wave expansion. The final column represents the rotational mole fractions of $H_2(v=1)$ at $T=310$ K. We note that although the JSA gives noticeable error, it is most accurate for the most populated state.

j	EXA	JSA	$p_{v=1,j}$
0	2.10	1.37	11.9%
1	1.98	2.23	63.6%
2	1.70	2.03	12.5%
3	1.31	0.976	11.2%

in addition to the respective mole fractions of the j states at $T=310$ K. We note that the JSA is very reliable at predicting the order of magnitude of the rate constants. However, there is noticeable error, ranging from -34.8% to $+19.4\%$. Furthermore, the JSA is poor at predicting the j dependence of the exact rate constants at this temperature, decreasing with increasing j. However, the scatter in error and the fact that the most populated j state is most accurately treated by the JSA suggests that it might do well to predict the average rate constant.

Table III shows the comparison between the CARS experiment, the present exact theory, and the JSA for the rotationally averaged rate constant at $T=310$ K, using the same units as in Table II. As hoped (and expected!), the exact theory agrees quantitatively with the experimental result. Thus, we can truly regard the determination of the $D+H_2(v=1)$ rate constant as a *solved problem* in gas-phase reaction dynamics. What is more intriguing, perhaps, is that the JSA predicts the rate constant quantitatively as well. Clearly, from the analysis of Table II, there is fortuitous cancellation of error in the average JSA rate constant. It is reasonable to question whether this cancellation is obtained at all temperatures, or only in this temperature range.

To answer this question, we have computed the rotationally averaged rate constant as a function of temperature, comparing exact theory to the JSA result. The common logarithm of the resulting rate constants is plotted in thick lines against inverse temperature in Fig. 3. In addition, the exact and JSA ($v=1$, $j=0$) selected rate constants are plotted in thin lines to demonstrate the systematic error. We see in Fig. 3 that the average JSA rate

TABLE III. Comparison between experiment, exact theory (EXA), and approximate theory (JSA) of rate constants for $D+H_2(v=1)$ at $T=310$ K ($10^{-13}\ \mathrm{cm}^3\ \mathrm{molecule}^{-1}\ \mathrm{s}^{-1}$). The theoretical values are obtained from Table II by averaging over the populated j states. The experimental value is from Dreier and Wolfrum (Ref. 21). Both the EXA and JSA rate constants agree quantitatively with experiment.

Method	$k_{v=1}(T=310\ \mathrm{K})$
Experiment	1.9 ± 0.2
EXA theory	1.87
JSA theory	1.95

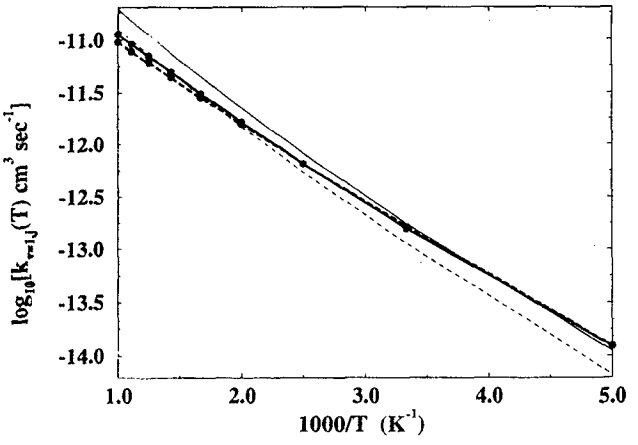

FIG. 3. Comparison between exact theory (*solid*) and the *J*-shifting approximation (JSA—*dash*) of $D+H_2(v=1, j)$ rate constants for $\langle j \rangle$ (*thick*) and $j=0$ (*thin*) as a function of temperature. With respect to the $j=0$ rate constants, the JSA consistently underestimates the exact rate constant by ~35%. However, with respect to the $\langle j \rangle$ rate constants, the JSA is nearly exact at the lower temperatures $T \leqslant 700$ K, and is semiquantitative throughout the entire temperature range. Noticeable error occurs at the highest temperatures as the assumptions inherent in the JSA break down.

constant quantitatively predicts the exact one up to $\sim T = 700$ K. At higher temperatures, the assumptions inherent in the JSA will naturally tend to break down, as is manifest in Fig. 3. Thus, we have shown that for this system, the JSA gives the correct order of magnitude for the more detailed $[v=1, j=(0,1,2,3)]$ selected rate constants, and is semiquantitative for the less detailed $(v=1, \langle j \rangle)$ selected rate constant.

V. CONCLUDING REMARKS

We have described the absorbing boundary condition (ABC) discrete variable representation (DVR) Newton method for carrying out efficient large-scale quantum reactive scattering calculations. The ABC-DVR Newton algorithm has been applied to the nontrivial problem of determining accurate reaction cross sections for $D+H_2(v=1, j)$ over a wide energy range. These cross sections were found to have very smooth energy dependence, and to systematically decrease with increasing j. In favorable circumstances, the present method gives converged reaction cross sections in 10 min on an IBM RS/6000 Model 550. In the most challenging cases, the calculations required no more than 60 min per energy (for $j=0$). In all cases, the core memory required was less than 4.5 Mbyte. We believe that the ABC-DVR Newton method has all the necessary ingredients to move exact quantum reactive scattering calculations past the three-atom problem.

The rate constants $k_{v=1,j}(T)$ were computed and thermally averaged over $j=(0,1,2,3)$ at $T=310$ K to model the experiment by Dreier and Wolfrum.[21] Our result is $k_{v=1}(T=310\text{ K}) = 1.87\times10^{-13}$ cm^3 molecule^{-1} s^{-1}, in *quantitative* agreement with their value $(1.9\pm0.2)\times10^{-13}$ cm^3 molecule^{-1} s^{-1}. We thus consider the subject of the $D+H_2(v=1)$ rate constant to be solved, with experiment and theory in complete agreement.

The *J*-shifting approximation (JSA) was tested against the exact $k_{v=1,j}(T)$ and $k_{v=1}(T)$ rate constants for $T=200$–1000 K. The $[v=1, j=(0,1,2,3)]$ selected JSA rate constants were qualitatively correct, but were in error by as much as 41%. The error systematically cancelled for the $(v=1, \langle j \rangle)$ selected rate constant, giving a semiquantitative description of this averaged quantity for $T \leqslant 700$ K.

Although the most detailed attributes of the $D+H_2$ reaction are still under discussion, e.g., the geometric phase,[4] we can confidently say that the average behavior of this system is well understood. We will apply the present methodology to elucidating such behavior in more complex reactive systems.

ACKNOWLEDGMENTS

S. M. A. thanks Professor Claude Leforestier for several helpful suggestions regarding the grid method. This work was supported under the Director, Office of Energy Research, Office of Basic Energy Sciences, Chemical Sciences Division of the U. S. Department of Energy under Contract No. DE-AC03-76SF00098.

[1] R. E. Continetti, B. A. Balko, and Y. T. Lee, J. Chem. Phys. **93**, 5719 (1990).
[2] R. E. Continetti, J. Z. H. Zhang, and W. H. Miller, J. Chem. Phys. **93**, 5356 (1990).
[3] D. Neuhauser, R. S. Judson, D. J. Kouri, D. A. Adelman, N. E. Shafer, D. A. V. Kliner, and R. N. Zare, Science **257**, 519 (1992).
[4] A. Kuppermann and Y.-S. M. Wu, Chem. Phys. Lett. **205**, 577 (1993).
[5] W. H. Miller and J. Z. H. Zhang, J. Phys. Chem. **95**, 12 (1991).
[6] For a recent review, see W. H. Miller, Annu. Rev. Phys. Chem. **41**, 245 (1990).
[7] For the first exact four-atom reactive scattering calculation, see U. Manthe, T. Seideman, and W. H. Miller, J. Chem. Phys. (in press).
[8] A. Sinha, M. C. Hsiao, and F. F. Crim, J. Chem. Phys. **94**, 4928 (1991).
[9] T. Seideman and W. H. Miller, J. Chem. Phys. **96**, 4412 (1992); **97**, 2499 (1992).
[10] W. H. Miller, Acc. Chem. Res. **26**, 174 (1993).
[11] D. Neuhauser and M. Baer, J. Chem. Phys. **91**, 4651 (1989).
[12] W. H. Thompson and W. H. Miller, Chem. Phys. Lett. **206**, 123 (1993).
[13] D. Neuhauser, R. S. Judson, R. L. Jaffe, M. Baer, and D. J. Kouri, Chem. Phys. Lett. **176**, 546 (1991).
[14] D. M. Young, Comput. Phys. Commun. **53**, 1 (1989).
[15] S. M. Auerbach and C. Leforestier, Comput. Phys. Commun. (to be published).
[16] J. Stoer and R. Bulirsch, *Introduction to Numerical Analysis* (Springer, New York, 1980).
[17] M. Berman, R. Kosloff, and H. Tal-Ezer, J. Phys. A **25**, 1283 (1992).
[18] M. Keuba, U. Wellhausen, and J. Wolfrum, Ber. Bunsenges. Phys. Chem. **83**, 940 (1979).
[19] G. P. Glass and B. K. Chaturvedi, J. Chem. Phys. **77**, 3478 (1982).
[20] V. B. Rozenshtegn, Yu. M. Gershenzon, A. V. Ivanov, and S. I. Kucheryavii, Chem. Phys. Lett. **105**, 423 (1984).
[21] T. Dreier and J. Wolfrum, Int. J. Chem. Kinet. **18**, 919 (1986).
[22] H. R. Mayne and J. P. Toennies, J. Chem. Phys. **75**, 1794 (1981).
[23] N. Abu Salbi, D. J. Kouri, Y. Shima, and M. Baer, J. Chem. Phys. **82**, 2650 (1985).
[24] E. Pollack, N. Abu Salbi, and D. J. Kouri, Chem. Phys. Lett. **113**, 585 (1985).
[25] J. C. Sun, B. H. Choi, R. T. Poe, and K. T. Tang, Phys. Rev. Lett. **44**, 1211 (1980).
[26] R. B. Walker and E. F. Hayes, J. Phys. Chem. **87**, 1255 (1983).
[27] E. Pollack, J. Chem. Phys. **82**, 106 (1985).

[28] B. C. Garrett and D. G. Truhlar, J. Phys. Chem. **89**, 2204 (1985).
[29] J. M. Bowman, K. T. Lee, and R. B. Walker, J. Chem. Phys. **79**, 3742 (1983).
[30] J. Z. H. Zhang and W. H. Miller, J. Chem. Phys. **91**, 1528 (1989).
[31] J. M. Bowman, J. Phys. Chem. **95**, 4960 (1991).
[32] J. V. Micheal, J. R. Fisher, J. M. Bowman, and Q. Y. Sun, Science **249**, 269 (1990).
[33] The JSA is essentially a molecular version of the modified wave number approximation of atomic physics. For this perspective, see K. Takayanagi, Prog. Theor. Phys. **8**, 497 (1952); E. E. Nikitin, *Elementary Theory of Atomic and Molecular Processes in Gases*, translated by M. J. Kearsley (Oxford University, New York, 1974), pp. 58–60.
[34] D. C. Chatfield, R. S. Friedman, D. G. Truhlar, B. C. Garrett, and D. W. Schwenke, J. Am. Chem. Soc. **113**, 486 (1991).
[35] S. Takada, A. Ohsaki, and H. Nakamura, J. Chem. Phys. **96**, 339 (1992).
[36] M. J. Bronikowski, W. R. Simpson, B. Girard, and R. N. Zare, J. Chem. Phys. **95**, 8647 (1991).
[37] R. D. Levine and R. B. Bernstein, *Molecular Reaction Dynamics and Chemical Reactivity* (Oxford University, New York, 1987).
[38] A. Goldberg and B. W. Shore, J. Phys. B **11**, 3339 (1978).
[39] C. Leforestier and R. E. Wyatt, J. Chem. Phys. **78**, 2334 (1983).
[40] R. Kosloff and D. Kosloff, J. Comput. Phys. **63**, 363 (1986).
[41] D. O. Harris, G. G. Engerholm, and W. D. Gwinn, J. Chem. Phys. **43**, 1515 (1965).
[42] A. S. Dickinson and P. R. Certain, J. Chem. Phys. **49**, 4209 (1968).
[43] J. C. Light, I. P. Hamilton, and J. V. Lill, J. Chem. Phys. **82**, 1400 (1985).
[44] For a brief review of modern numerical methods in sparse linear system solving, see S. M. Auerbach and W. H. Miller, J. Chem. Phys. **98**, 6917 (1993).
[45] H. Tal-Ezer and R. Kosloff, J. Chem. Phys. **81**, 3967 (1984).
[46] M. Abramowitz and I. A. Stegun, *Handbook of Mathematical Functions with Formulas, Graphs, and Mathematical Tables* (Wiley, New York, 1972).
[47] C. Lanczos, J. Res. Natl. Bur. Stand. **45**, 255 (1950).
[48] S. E. Choi and J. C. Light, J. Chem. Phys. **92**, 2129 (1990).
[49] R. T Pack, J. Chem. Phys. **60**, 633 (1974).
[50] J. Z. H. Zhang, J. Chem. Phys. **94**, 6047 (1991).
[51] M. E. Rose, *Elementary Theory of Angular Momentum* (Wiley, New York, 1967).
[52] P. Siegbahn and B. Liu, J. Chem. Phys. **68**, 2457 (1978).
[53] D. G. Truhlar and C. J. Horowitz, J. Chem. Phys. **68**, 2466 (1978).
[54] D. G. Truhlar and C. J. Horowitz, J. Chem. Phys. **71**, 1514(E) (1979).
[55] G. C. Groenenboom, Report, Netherlands Organization for Scientific Research (NWO) (1992).
[56] G. C. Groenenboom and D. T. Colbert, J. Chem. Phys. (in press).
[57] D. T. Colbert and W. H. Miller, J. Chem. Phys. **96**, 1982 (1992).
[58] C. Leforestier, J. Chem. Phys. **94**, 6388 (1991).
[59] G. C. Corey and D. Lemoine, J. Chem. Phys. **97**, 4115 (1992).
[60] Z. Bačić and J. C. Light, J. Chem. Phys. **85**, 4594 (1986).
[61] W. H. Miller, J. Chem. Phys. **49**, 2373 (1968).
[62] D. Neuhauser and M. Baer, J. Chem. Phys. **90**, 4351 (1989).
[63] M. S. Child, Mol. Phys. **72**, 89 (1991).
[64] Á. Vibók and G. G. Balint-Kurti, J. Phys. Chem. **96**, 8712 (1992).
[65] Á. Vibók and G. G. Balint-Kurti, J. Chem. Phys. **96**, 7615 (1992).
[66] Q. Sun, J. M. Bowman, G. C. Schatz, J. R. Sharp, and J. L. Connor, J. Chem. Phys. **92**, 1677 (1990).
[67] M. C. Colton and G. C. Schatz, Int. J. Chem. Kinet. **18**, 961 (1986).